Generation of σ,π-furyl and thienyl ligands at di-iron centers via facile phosphorus–carbon bond cleavage: Synthesis and molecular structures of [Fe2(CO)6(μ-η1,η2-C4H3E){μ-P(C4H3E)...

ARTICLE *in* JOURNAL OF ORGANOMETALLIC CHEMISTRY · APRIL 2013

Impact Factor: 2.17 · DOI: 10.1016/j.jorganchem.2012.11.024

Journal of Organometallic Chemistry 730 (2013) 123–131

Contents lists available at SciVerse ScienceDirect

Journal of Organometallic Chemistry

journal homepage: www.elsevier.com/locate/jorganchem

Generation of σ,π-furyl and thienyl ligands at di-iron centers *via* facile phosphorus–carbon bond cleavage: Synthesis and molecular structures of $[Fe_2(CO)_6(\mu\text{-}\eta^1,\eta^2\text{-}C_4H_3E)\{\mu\text{-}P(C_4H_3E)_2\}]$ (E = O, S)☆

Ahibur Rahaman [a,b], Fakir Rafiqul Alam [b,c], Shishir Ghosh [b,d], Matti Haukka [e], Shariff E. Kabir [b,**], Ebbe Nordlander [a,***], Graeme Hogarth [d,*]

[a] Inorganic Chemistry Research Group, Chemical Physics, Center for Chemistry and Chemical Engineering, Lund University, Box 124, SE-221 00 Lund, Sweden
[b] Department of Chemistry, Jahangirnagar University, Savar, Dhaka 1342, Bangladesh
[c] Department of Chemistry, National University, Gazipur 1704, Bangladesh
[d] Department of Chemistry, University College London, 20 Gordon Street, London WC1H OAJ, UK
[e] Department of Chemistry, University of Jyveskylä, Box 111, FI-40014, Jyväskylä, Finland

ARTICLE INFO

Article history:
Received 3 October 2012
Received in revised form
15 November 2012
Accepted 18 November 2012

Keywords:
Phosphine
Tri-iron
Di-iron
Carbon–phosphorus bond scission
Furyl
Thienyl

ABSTRACT

Treatment of $[Fe_3(CO)_{12}]$ with tri(2-furyl)phosphine (PFu_3) or tri(2-thienyl)phosphine (PTh_3) in dichloromethane at 40 °C leads to facile phosphorus–carbon bond scission affording di-iron furyl- and thienyl-bridged complexes $[Fe_2(CO)_6(\mu\text{-}\eta^1,\eta^2\text{-}C_4H_3E)\{\mu\text{-}P(C_4H_3E)_2\}]$ (**1** E = O, Fu; **3** E = S, Th) in good yields, together with smaller amounts of the phosphine-substituted $[Fe_2(CO)_5(\mu\text{-}\eta^1,\eta^2\text{-}C_4H_3E)\{\mu\text{-}P(C_4H_3E)_2\}\{P(C_4H_3E)_3\}]$ (**2** E = O, **4** E = S). When the same reactions were carried out at room temperature, small amounts of the tri-iron clusters $[Fe_3(CO)_{11}\{P(C_4H_3E)_3\}]$ (**5** E = O, **6** E = S) were isolated in which the coordinated phosphine(s) remain intact. Thermolysis of $[Fe_3(CO)_{11}\{P(C_4H_3E)_3\}]$ at 40 °C in dichloromethane gave $[Fe_2(CO)_6(\mu\text{-}\eta^1,\eta^2\text{-}C_4H_3E)\{\mu\text{-}P(C_4H_3E)_2\}]$, which also undergo phosphine substitution under similar conditions. However, both of these processes are too slow to account for the reaction product ratios and yields observed in the room temperature reactions. In contrast, addition of catalytic amounts of $Na^+[Ph_2CO]^\bullet$ to **5** resulted in the rapid formation of **1**. We therefore propose that these reactions may occur *via* a radical-initiated mechanism proceeding through the initial formation of the 49-electron radical anions $[Fe_3(CO)_{11}\{P(C_4H_3E)_3\}]^\bullet$. The crystal structures of $[Fe_2(CO)_6(\mu\text{-}\eta^1,\eta^2\text{-}Fu)(\mu\text{-}PFu_2)]$ (**1**), $[Fe_2(CO)_5(\mu\text{-}\eta^1,\eta^2\text{-}Fu)(\mu\text{-}PFu_2)(PFu_3)]$ (**2**), $[Fe_2(CO)_6(\mu\text{-}\eta^1,\eta^2\text{-}Th)(\mu\text{-}PTh_2)]$ (**3**) and $[Fe_3(CO)_{11}(PFu_3)]$ (**5**) have been determined. The di-iron complexes all show the expected *cis* arrangement of three-electron donor ligands, short iron–iron distances consistent with a 34-valence electron count, and, in **2**, the phosphine is coordinated to the π-bound iron atom and lies *trans* to the metal–metal bond. Close inspection of the bonding parameters within the Fe_2C_2E core reveals that these alkenyl species are quite different to those without electron-withdrawing substituents. The tri-iron cluster **5** has two independent molecules in the asymmetric unit. Each contains two bridging carbonyls and the molecules differ in the relative positions of these carbonyls and the coordinated phosphine ligand, the latter lying in the equatorial plane in both molecules.

1. Introduction

The organometallic chemistry of tri(2-furyl)phosphine (PFu_3) [1–18] and tri(2-thienyl)phosphine (PTh_3) [19–29] has been extensively developed over the past decade. Sterically they are somewhat similar to triphenylphosphine; however, the electron-withdrawing nature of the 2-heteroaryl rings is greater than that of the phenyl ring, which makes PFu_3 and PTh_3 poorer σ-donors than PPh_3 [30]. This has been exploited in certain catalytic reactions, with PFu_3-containing catalysts often being more active than traditional PPh_3-based catalysts [3–9].

While in the majority of instances PFu_3 and PTh_3 act simply as two-electron donor ligands, a second reactivity pattern is the relatively facile carbon–phosphorus bond cleavage leading to phosphido and furyl/thienyl moieties [1,11–16,20,23,27,29] (Scheme 1). Thus Wong and co-workers prepared dinuclear

☆ In memory of Professor F.G.A. Stone FRS, a leading protagonist of low-valent transition metal cluster chemistry and an inspiration to us all.

* Corresponding author.
** Corresponding author.
*** Corresponding author.
E-mail address: g.hogarth@ucl.ac.uk (G. Hogarth).

0022-328X/$ – see front matter © 2012 Elsevier B.V. All rights reserved.
http://dx.doi.org/10.1016/j.jorganchem.2012.11.024

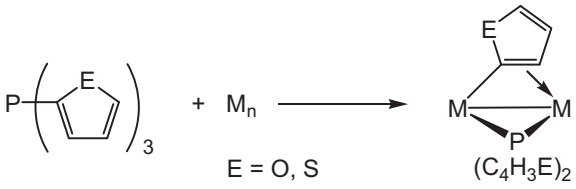

Scheme 1.

$[Ru_2(CO)_6(\mu\text{-}\eta^1,\eta^2\text{-Fu})(\mu\text{-}PFu_2)]$ from the reaction of $[Ru_3(CO)_{12}]$ with PFu_3 at 67 °C in which the heteroaromatic group is bound to the bimetallic framework in a σ,π-alkenyl fashion [15]. In developing the use of PFu_3 as a source of a furyl ligand, we have recently shown that this transformation occurs *via* initial coordination of PFu_3 to the triruthenium center, as heating $[Ru_3(CO)_{12-n}(PFu_3)_n]$ ($n = 2, 3$) affords the same complex [16], while a similar thermolysis of $[Ru_3(CO)_9(PFu_3)_3]$ in the presence of Me_3NO affords $[Ru_2(CO)_5(PFu_3)(\mu\text{-}PFu_2)(\mu\text{-}\eta^1,\eta^2\text{-Fu})]$ [16]. In seeking to further utilise this facile carbon–phosphorus bond scission to prepare related di-iron furyl and thienyl complexes, we herein report reaction of $[Fe_3(CO)_{12}]$ with PFu_3 and PTh_3, and show that phosphorus–carbon bond cleavage is very facile at the tri-iron center, leading to the facile formation of di-iron furyl- and thienyl-bridged complexes, which is proposed to occur *via* a radical-initiated mechanism.

2. Results and discussion

2.1. Thermolysis of $[Fe_3(CO)_{12}]$ with PFu_3 and PTh_3 – synthesis of σ,π-alkenyl complexes via carbon–phosphorus bond scission

Refluxing a dichloromethane solution of $[Fe_3(CO)_{12}]$ and PFu_3 for 12 h led to the isolation of the di-iron complexes $[Fe_2(CO)_6(\mu\text{-}\eta^1,\eta^2\text{-Fu})(\mu\text{-}PFu_2)]$ (**1**) and $[Fe_2(CO)_5(\mu\text{-}\eta^1,\eta^2\text{-Fu})(\mu\text{-}PFu_2)(PFu_3)]$ (**2**) after chromatography, in yields of 59 and 12%, respectively. The same reaction with PTh_3 gave primarily $[Fe_2(CO)_6(\mu\text{-}\eta^1,\eta^2\text{-Th})(\mu\text{-}PTh_2)]$ (**3**) (72%) together with small amounts of phosphine-substituted $[Fe_2(CO)_5(\mu\text{-}\eta^1,\eta^2\text{-Th})(\mu\text{-}PTh_2)(PTh_3)]$ (**4**) (2%) (Scheme 2).

Characterisation of these new complexes was straightforward. The IR spectra of **1** and **2** show four terminal carbonyl bands, the patterns being characteristic of an $Fe_2(CO)_6(\mu\text{-X})(\mu\text{-Y})$ core (where X and Y are different three-electron donor ligands). Cleavage of a carbon–phosphorus bond leading to the generation of a phosphido-bridge could be established from the $^{31}P\{^1H\}$ NMR spectrum. Thus **1** displays a low-field singlet at 91.7 ppm as compared to −75.8 ppm for the free phosphine ligand, while in **3** the phosphido signal is shifted to even lower field, appearing at 113.0 ppm. For **2** and **4** the IR spectra are consistent with a di-iron pentacarbonyl core and the $^{31}P\{^1H\}$NMR spectra did again provide the most useful characterizing data. Thus the spectrum of **2** consists of doublets at 80.9 and 21.3 ppm, assigned to the phosphido and coordinated intact phosphine ligands, respectively, the phosphorus–phosphorus coupling constant of 29.1 Hz suggesting a relative *cis* disposition of the two ligands. A similar spectrum is observed for **4**, consisting of doublets at 75.9 and 23.2 ppm ($J_{PP} = 26.2$ Hz).

In order to confirm the nature of the phosphorus–carbon bond cleavage process and also determine the relative positions of the phosphido and coordinated phosphine ligands, the crystal structures of **1**–**3** were determined. The molecular structures are shown in Figs. 1 and 2; relevant bond distances and angles are summarized in Table 1. The latter also contains some key metric data for related diphenylphosphido-bridged complexes and the parameters ΔC_α and ΔFe_π, defined as $\{(Fe_\pi\text{–}C_\alpha)\text{–}(Fe_\sigma\text{–}C_\alpha)\}$ and $\{(Fe_\pi\text{–}C_\alpha)\text{–}(Fe_\pi\text{–}C_\beta)\}$, respectively [31], with ΔC_α being a measure of how symmetrically the α-carbon bridges the di-iron centre and ΔFe_π differentiating between metallaolefin and metallacyclic binding modes [31]. For **2** there are two independent molecules in the asymmetric unit (Fig. 2). They differ primarily in the relative positions of the furyl groups on the phosphido-bridge. Otherwise the structures are very similar with only minor variations in bond lengths and angles.

All three complexes contain the same di-iron-phosphido-furyl/thienyl framework, with the two three-electron donor phosphido and furyl/thienyl ligands lying *cis* to one another, as expected. The metric parameters within the three complexes are similar to those in related σ,π-alkenyl complexes (Table 1). The iron–iron bond lengths vary only slightly within this series, as has been previously noted in a large number of alkenyl-bridged di-iron complexes [31–44]. Likewise, there is little variation in the carbon–carbon bond length in the alkenyl moiety, those in **1**–**3** of 1.405(7)–1.409(4) Å being typical. More interesting are the bond lengths between the alkenyl and di-iron centre. In all three structures, the α-carbon atom bridges the di-iron centre in a highly unsymmetrical fashion that arises as a result of both the relatively short $Fe_\sigma\text{–}C_\alpha$ and long $Fe_\pi\text{–}C_\alpha$ distances. The ΔC_α values thus vary between 0.172(4) and 0.223(4) Å, as compared to more typical values of around 0.1 Å. Bonds to the β-carbon are also long, with $Fe_\pi\text{–}C_\beta$ varying between 2.269(3) and 2.370(4) Å, some 0.1 Å longer than in related alkenyl complexes. The lengthening of both of the Fe_π–C bonds results in ΔFe_π values of 0.094(4)–0.173(7) Å, being similar to those seen previously. As observed in related complexes, the binding of the phosphido-bridge is slightly unsymmetrical, with the bonds to Fe_σ being consistently shorter than those to Fe_π. The most significant feature of **2** is the position of the phosphine ligand which is bound to the π-bound iron centre and lies approximately *trans* to the iron–iron bond [P(1)–Fe(2)–P(2) 156.22(3)–156.51(3)°]. It sits at approximately right angle to the phosphido-bridge and the angles subtended between the two phosphorus atoms [P(1)–Fe(2)–P(2) 105.89(3), P(3)–Fe(4)–P(4) 104.55(3)°] are in accord with the relatively small phosphorus–phosphorus coupling constants observed in solution. The structural features seen for **2** are very similar to those found in the analogous ruthenium complex $[Ru_2(CO)_5(\mu\text{-}\eta^1,\eta^2\text{-Fu})(\mu\text{-}PFu_2)(PFu_3)]$ (**2-Ru**, cf. Table 1) [16]. Table 1 also presents metric parameters for $[Ru_2(CO)_6(\mu\text{-}\eta^1,\eta^2\text{-Fu})(\mu\text{-}PFu_2)]$ (**1-Ru**) [15,16] and $[Ru_2(CO)_5(\mu\text{-}\eta^1,\eta^2\text{-Fu})(\mu\text{-}PFu_2)(PFu_3)]$ (**2-Ru**) [16]. In general, the structures differ only slightly upon exchange of iron for ruthenium, but there are some important subtle differences that are

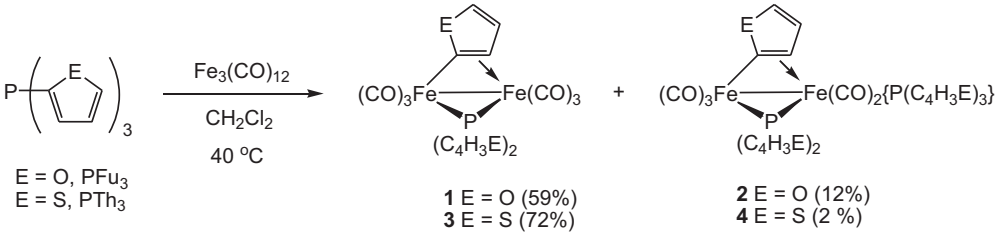

Scheme 2.

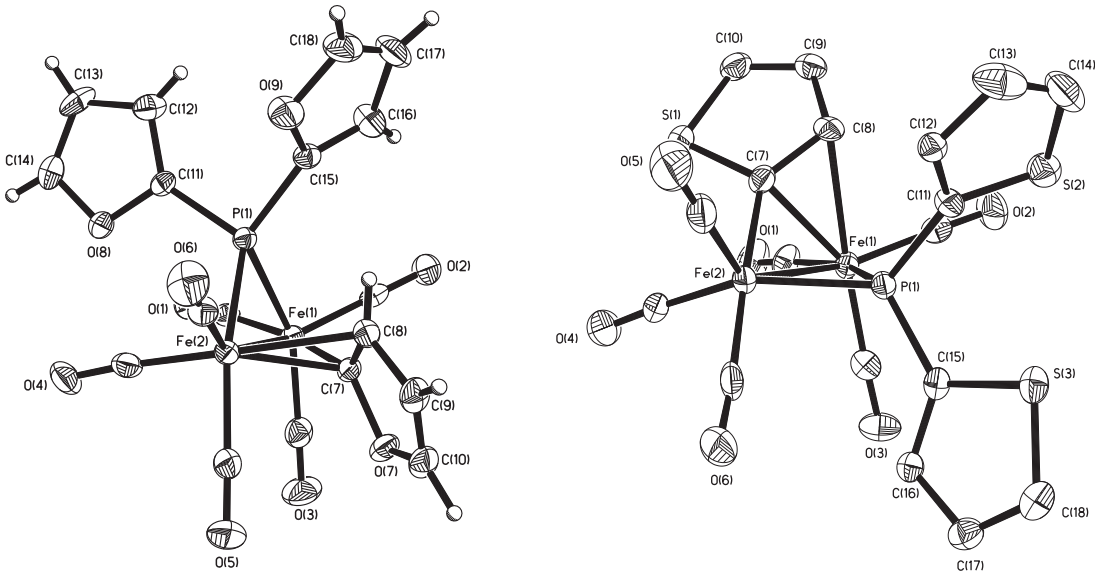

Fig. 1. Molecular structures of $[Fe_2(CO)_6(\mu\text{-}\eta^1,\eta^2\text{-Fu})(\mu\text{-}PFu_2)]$ (**1**) and $[Fe_2(CO)_6(\mu\text{-}\eta^1,\eta^2\text{-Th})(\mu\text{-}PTh_2)]$ (**3**).

consequences of the different atomic (ionic) radii of the metal atoms. Notably, the ΔC_α values for **1-Ru** (0.296 Å) and **2-Ru** (0.230 Å) are significantly larger than those for **1** (0.205 Å) and **2** (0.198 Å av.), while ΔRu_π values of 0.046 and 0.070 Å for **1-Ru** and **2-Ru**, respectively, compare with those of 0.155 and 0.116 Å (av.) for the related iron complexes. Both of these differences result primarily from the longer Ru_π–C_α bonds found in the ruthenium complexes.

The facile cleavage of phosphorus–carbon bonds at a di-iron centre is quite common [45–51]. Most closely related to the work described here is the formation of $[Fe_2(CO)_4(\mu\text{-}PPh_2)(\mu\text{-}HC{=}CH_2)(\mu\text{-}Ph_2PCH_2PPh_2)]$ upon reaction of $Ph_2PCH{=}CH_2$ with $[Fe_2(CO)_6(\mu\text{-}CO)(\mu\text{-}Ph_2PCH_2PPh_2)]$ [51], a process in which both the phosphine and alkene groups are metal-bound prior to bond scission.

2.2. Room temperature reactions of $[Fe_3(CO)_{12}]$ with PFu_3 and PTh_3 – isolation of tri-iron complexes with coordinated phosphines

In order to gain more insight into the nature of the transformations described above we carried out the reactions of PFu_3 and PTh_3 with $[Fe_3(CO)_{12}]$ at room temperature in an attempt to identify and isolate expected tri-iron intermediates. Treatment of $[Fe_3(CO)_{12}]$ with PFu_3 at room temperature in dichloromethane afforded after chromatographic work-up three isolated products: the previously discussed di-iron complexes **1** and **2** were the major products that were isolated in 57 and 11% yields, respectively, together with small amounts of green $[Fe_3(CO)_{11}(PFu_3)]$ (**5**) (6%). Similarly, with PTh_3 the major products were still the two di-iron complexes 3 and 4 (58 and 2% yields respectively) were still formed together with $[Fe_3(CO)_{11}(PTh_3)]$ (**6**) (7% yield) (Scheme 3).

The colour of **5** and **6** is strongly indicative of a tri-iron core and their IR spectra are quite distinctive from those of the di-iron alkenyl species. In order to confirm the nature of these species, the crystal structure of $[Fe_3(CO)_{11}(PFu_3)]$ (**5**) was determined. The molecular structure of **5** is shown in Fig. 3 and relevant metric data are summarized in Table 2. The complex crystallizes with two independent molecules, which are structural isomers, in the asymmetric unit. This phenomenon was also observed for the analogue $[Fe_3(CO)_{11}(PPh_3)]$ [52] and in both instances the two isomers differ by the location of the phosphine ligand within the

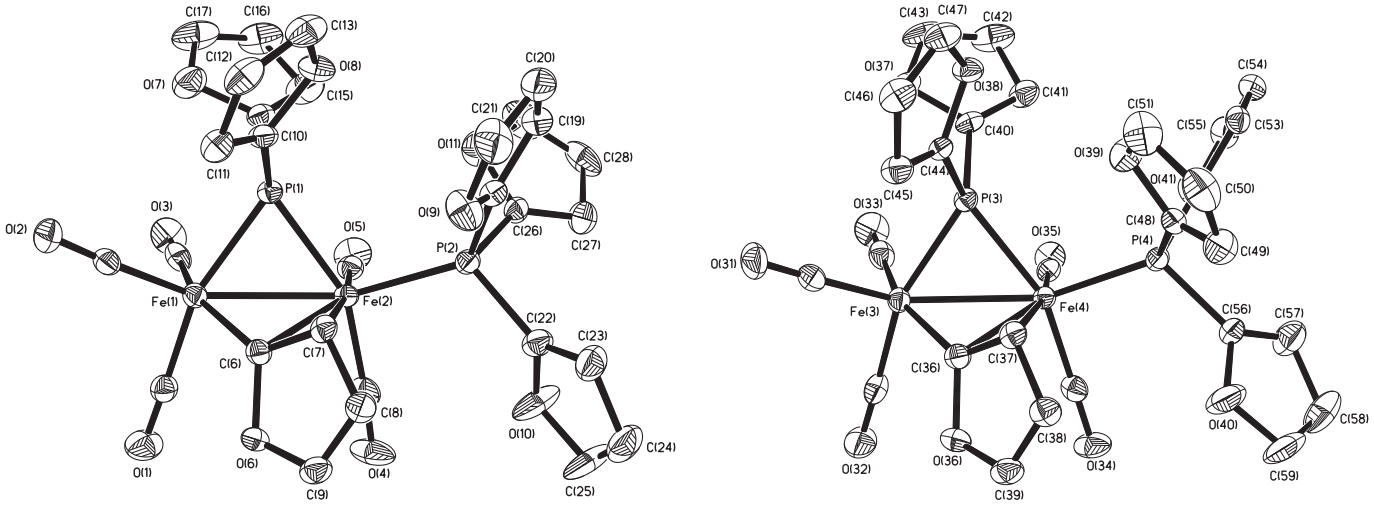

Fig. 2. Molecular structures of the two independent molecules of $[Fe_2(CO)_5(\mu\text{-}\eta^1,\eta^2\text{-Fu})(\mu\text{-}PFu_2)(PFu_3)]$ (**2**).

Table 1
Selected bond lengths (Å) and angles (°) for **1**–**3** and the related di-iron–alkenyl complexes $[Fe_2(CO)_6(\mu\text{-}PPh_2)(\mu\text{-}R_1C{=}CHR_2)]$ and $[Ru_2(CO)_6(\mu\text{-}PFu_2)(\mu\text{-}Fu)]$ (**1-Ru**) and $[Ru_2(CO)_5(PFu_3)(\mu\text{-}PFu_2)(\mu\text{-}Fu)]$ (**2-Ru**).

Compound	Fe–Fe	Fe_σ–C_α	Fe_π–C_α	Fe_π–C_β	C_α–C_β	ΔC_α[b]	ΔFe_π[c]	Fe–C_α–Fe	Fe_σ–PR_2	Fe_π–PR_2	Fe–P–Fe	Fe_β–PR_3	Fe_α–Fe_β–PR_3	Reference
1	2.6056(6)	1.947(3)	2.152(2)	2.307(3)	1.406(4)	0.205	0.155	78.77(9)	2.1997(9)	2.2278(9)	72.10(2)			This work
2[a]	2.5922(7)	1.952(3)	2.175(3)	2.269(3)	1.409(4)	0.223	0.094	77.6(1)	2.2139(9)	2.2310(9)	71.35(3)	2.1988(9)	156.51(3)	This work
	2.5938(6)	1.961(3)	2.133(3)	2.272(3)	1.409(4)	0.172	0.139	78.5(1)	2.2094(9)	2.2390(9)	71.33(3)	2.1931(9)	156.22(3)	
3	2.6168(9)	1.978(5)	2.197(5)	2.370(4)	1.405(7)	0.219	0.173	77.4(2)	2.196(1)	2.238(1)	72.33(4)			This work
$R_1 = R_2 = H$	2.597(1)	1.964(2)	2.084(3)	2.169(3)	1.379(5)	0.120	0.085	–	2.215(1)	2.258(1)	71.0(1)			[33]
$R_1 = R_2 = Ph$	2.597(1)	2.038(10)	2.099(7)	2.223(7)	1.424(13)	0.061	0.124	77.7(3)	2.223(2)	2.260(1)	–			[32]
$R_1 = Ph$, $R_2 = H$	2.615(1)	2.007(5)	2.109(5)	2.165(6)	1.393(8)	0.102	0.056	78.8(2)	2.229(2)	2.252(2)	71.43(5)			[31]
$R_1 = H$, $R_2 = Ph$	2.617(1)	1.996(4)	2.119(4)	2.269	1.405(5)	0.123	0.150	78.9(1)	2.251(1)	2.294(1)	70.29(4)			[31]
	Ru–Ru	Ru_σ–C_α	Ru_π–C_α	Ru_π–C_β	C_α–C_β	ΔC_α	ΔRu_π	Ru–C_α–Ru	Ru_σ–PR_2	Ru_π–PR_2	Ru–P–Ru	Ru_β–PR_3	Ru_α–Ru_β–PR_3	
1-Ru	2.7695(3)	2.071(2)	2.367(2)	2.413(2)		0.296	0.046		2.3228(6)	2.3418(6)	72.84(2)			[16]
2-Ru	2.7711(3)	2.078(2)	2.308(2)	2.378(2)		0.230	0.070		2.3304(5)	2.3595(5)	72.44(2)	2.3068(6)	154.98(2)	[16]

[a] Two independent molecules in the asymmetric unit.
[b] $\Delta C_\alpha = (Fe_\pi\text{–}C_\alpha) - (Fe_\sigma\text{–}C_\alpha)$.
[c] $\Delta Fe_\pi = (\ Fe_\pi\text{–}C_\alpha) - (\ Fe_\pi\text{–}C_\beta)$.

cluster framework. In both molecules of **5**, one iron–iron edge is bridged by two carbonyls and the phosphine ligand is bound to one of these iron atoms in one molecule (**5b**, Fig. 3b), whereas it is bound to the remote iron atom in the other (**5a**, Fig. 3a). Somewhat surprisingly, the metric parameters, especially bond lengths, resemble those in $[Fe_3(CO)_{12}]$ more closely than those in $[Fe_3(CO)_{11}(PPh_3)]$ (Table 2). As expected, the carbonyl-bridged iron–iron edge is much shorter than both non-bridged iron–iron vectors in both molecules of **5**, and the iron–iron distances are very similar to those in $[Fe_3(CO)_{12}]$ but are slightly shorter than those found in $[Fe_3(CO)_9(\mu\text{-}CO)_2(PPh_3)]$. All three iron–iron bonds in **5b** are slightly longer (~0.03 Å) than those in $[Fe_3(CO)_{12}]$. Calculations suggest that the carbonyl ligands in $[Fe_3(CO)_{12}]$ remove much of the electron density from the iron–iron anti-bonding orbitals and thereby strengthen the iron–iron bonds [52]. In contrast, the relatively poor π-acceptor ligand PPh_3 cannot act in this manner and thus weakens the iron–iron bonds, as noted in their lengthening in $[Fe_3(CO)_{11}(PPh_3)]$. Since PFu_3 is a significantly better π-acceptor than PPh_3, it can more effectively remove electron density from the anti-bonding iron–iron orbitals, thus leading to a shortening of the metal vectors in **5**. For the same reason, the iron-phosphorus bond distances in **5** [Fe–P 2.2108(4) and 2.2147(4) Å] are significantly shorter than those in $[Fe_3(CO)_{11}(PPh_3)]$ [Fe–P 2.25(1) and 2.24(1) Å]. Notably, the carbonyl bridges are almost symmetric in **5a** [Fe(2)–C(7) 1.988(2), Fe(3)–C(7) 1.978(2), Fe(2)–C(8) 1.977(1), Fe(3)–C(8) 1.992(2) Å] but asymmetric in **5b** [Fe(2B)–C(7B) 1.904(1), Fe(3B)–C(7B) 2.098(2), Fe(2B)–C(8B) 2.011(1), Fe(3B)–C(8B) 1.938(1) Å]. In contrast, all carbonyl bridges within both independent molecules of $[Fe_3(CO)_{11}(PPh_3)]$ [52] and in $[Fe_3(CO)_{12}]$ are asymmetric [53,54].

Cluster **5** is soluble and stable in common organic solvents under a nitrogen atmosphere but decomposes slowly when exposed to air. Analytical and solution spectroscopic data are consistent with the formulation. The IR spectrum in cyclohexane shows weak absorptions at 1847 and 1807 cm^{-1} associated with the bridging carbonyls. The pattern of the IR spectrum is very similar to that of $[Fe_3(CO)_{11}(PPh_3)]$ [52] indicating that they are isostructural. The ^1H NMR spectrum is fully consistent with the solid state structure of **5** and the $^{31}P\{^1H\}$ NMR spectrum shows a singlet at 20.0 ppm. The FAB mass spectrum shows the molecular ion peak at *m/z* 708.80, a clear indication of its trinuclear nature. The tri(2-thienyl)phosphine analogue $[Fe_3(CO)_{11}(PTh_3)]$ (**6**) is spectroscopically very similar to **5**, showing weak absorption bands at 1840 and 1800 cm^{-1} in the IR spectrum and a singlet at 33.0 ppm in the $^{31}P\{^1H\}$ NMR spectrum.

2.3. Mechanistic insights

In order to gain further insight into the transformations described above we have carried out a series of experiments in order to ascertain an overall pathway for the synthesis of di-iron σ,π-furyl and thienyl complexes. In the related ruthenium chemistry, we have shown that initial binding of PFu_3 to the triruthenium core affords $[Ru_3(CO)_{11}(PFu_3)]$ and $[Ru_3(CO)_{10}(PFu_3)_2]$ which upon heating rearrange to give $[Ru_2(CO)_6(\mu\text{-}\eta^1,\eta^2\text{-}Fu)(\mu\text{-}PFu_2)]$ and $[Ru_2(CO)_5(\mu\text{-}\eta^1,\eta^2\text{-}Fu)(\mu\text{-}PFu_2)(PFu_3)]$, respectively [16]. Hence it seems probable that related tri-iron complexes are precursors to the dinuclear furyl and thienyl complexes described herein. However, the tri-iron complexes **5** and **6** were found to be stable in dichloromethane (and thf) at room temperature under a nitrogen atmosphere without evidence of phosphorus–carbon bond scission even after prolonged standing. Upon heating, however, they do transform into dinuclear furyl and thienyl products. Thus a refluxing dichloromethane solution of $[Fe_3(CO)_{11}(PFu_3)]$ (**5**) gave a mixture of **1** (35%) and **2** (15%), while heating $[Fe_3(CO)_{11}(PTh_3)]$ (**6**) for 6 h in dichloromethane afforded **3** (40%). Both these experiments show that carbon–phosphorus bond scission can occur at the tri-iron centre, but that activation barriers are relatively high. Similarly, carbonyl substitution at the di-iron centre is not facile under the reaction conditions. Thus, prolonged stirring of **1** and PFu_3 at room temperature did not lead to the formation of significant amounts of substitution product, while in refluxing

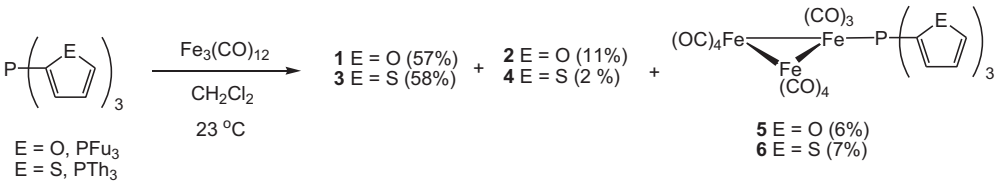

Scheme 3.

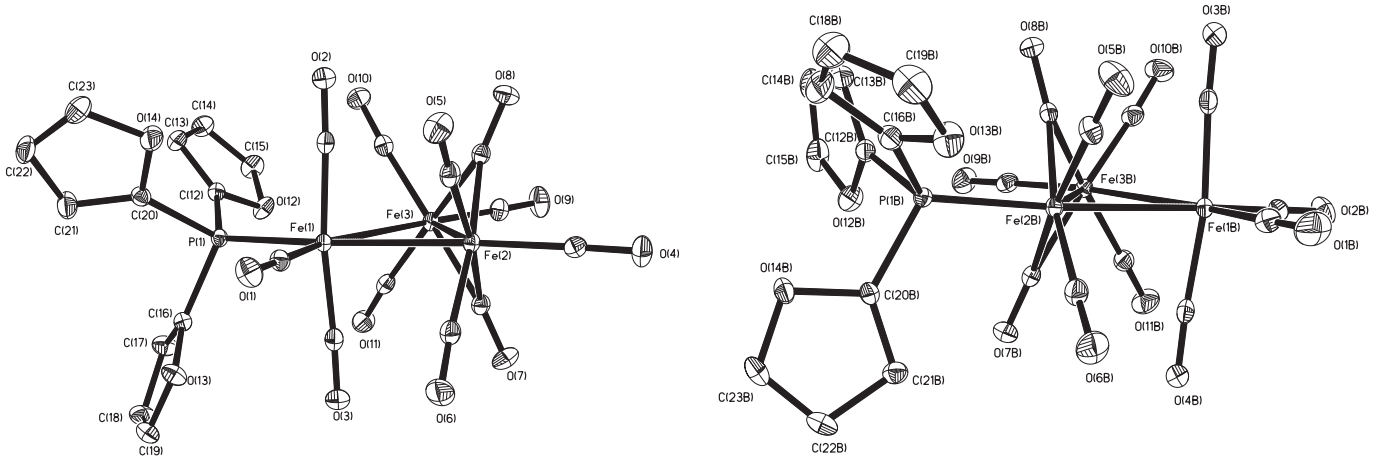

Fig. 3. Molecular structures of the two independent molecules of $[Fe_3(CO)_{11}(PFu_3)]$ (**5**); (a) **5a**, (b) **5b**.

dichloromethane **2** was generated in 10% yield after 6 h. This experiment shows that while **1** is a precursor to **2**, the latter must also be formed by a different route.

The substitution chemistry of $[Fe_3(CO)_{12}]$ is known to be extremely complex, being dependent upon factors such as the nature of the solvent and ligand concentrations. The reaction with PPh_3 has been studied by a number of groups [55–57]. In hexane [55] and benzene [56] both substitution and fragmentation take place at comparable rates. In thf, however, an electron-transfer mechanism has been proposed [57,58]. This involves the initial formation of the 49-electron radical anion, $[Fe_3(CO)_{12}]^{\bullet}$ [58–61], which rapidly loses CO to afford crystallographically characterized $[Fe_3(CO)_{11}]^{\bullet}$ [62], which in turn reacts with PPh_3 to yield $[Fe_3(CO)_{11}(PPh_3)]^{\bullet}$. The latter can lose an electron to afford the tri-iron product or undergo fragmentation to give the observed mononuclear products. The nature of the activating species was not fully discerned; however, when freshly purified PPh_3 was used the rate of reaction decreased, leading the authors to suggest that trace amounts of $Ph_3P{=}O$ may be responsible for the initial reduction of $[Fe_3(CO)_{12}]$. In light of this, we considered that reactions of $[Fe_3(CO)_{12}]$ with PFu_3 and PTh_3 may operate *via* free-radical initiation. We found that while $[Fe_3(CO)_{11}(PFu_3)]$ (**5**) is stable in thf at room temperature, addition of a small amount of $Na^+[Ph_2CO]^{\bullet}$ results in the rapid formation of $[Fe_2(CO)_6(\mu\text{-}\eta^1,\eta^2\text{-Fu})(\mu\text{-}PFu_2)]$ (**1**) in good yield (62%), suggesting that the conversion of **5**–**1** indeed proceeds *via* a free-radical-initiated reaction. We tentatively propose an overall reaction as shown in Scheme 4.

We postulate that the 49-electron radical anions $[Fe_3(CO)_{11}\{P(C_4H_3E)_3\}]^{\bullet}$ (**A**) are formed *via* initial formation of $[Fe_3(CO)_{12}]^{\bullet}$ followed by CO substitution by a phosphine, as documented by Cheng and co-workers [57]. Such species **A** can then undergo a number of different transformations. Transfer of an electron from **A** to $[Fe_3(CO)_{12}]$ would lead to formation of the observed tri-iron complexes $[Fe_3(CO)_{11}\{P(C_4H_3E)_3\}]$ (**5**–**6**). Presumably this is a relatively minor pathway, the dominant one being cluster fragmentation *via* loss of $[Fe(CO)_5]$ followed by coordination of a furyl or thienyl group through a carbon–carbon double bond to afford 33-electron radicals $[Fe_2(CO)_6\{\mu\text{-}P(C_4H_3E)_3\}]^{\bullet}$ (**B**). Such species can then lose an electron to form 32-electron complexes that would be susceptible to oxidative addition of a carbon–phosphorus bond to the di-iron centre to afford the observed products **1** and **3**, or undergo further carbonyl substitution, followed by electron loss to yield the substituted derivatives **2** and **4**. Another possible route to the latter is *via* the putative 49-electron radical anions $[Fe_3(CO)_{10}\{P(C_4H_3E)_3\}_2]^{\bullet}$, however, we note that such disubstituted phosphine complexes are rare [63] and $[Fe_3(CO)_{10}(PPh_3)_2]$ remains unknown. In the absence of the diphenyl ketyl anion radical, it is unclear what the source of free-radical initiation is. Two potential sources may be identified: (*i*) decomposition of dichloromethane – this solvent is known to degrade with time and alkanes are typically added as preservatives [64], (*ii*) the cluster, $[Fe_3(CO)_{12}]$, is prone to decomposition to elemental iron.

Table 2
Selected bond lengths (Å) and angles (°) for the two independent molecules of $[Fe_3(CO)_{11}(PFu_3)]$ (**5**) and $[Fe_3(CO)_{11}(PPh_3)]$, and $[Fe_3(CO)_{12}]$.

Compound	CO-Bridged Fe–Fe	Unbridged Fe–Fe 1	Unbridged Fe–Fe 2	Fe–P	Reference
5a	2.5476(3)	2.6894(3)	2.6955(3)	2.2108(4)	This work
5b	2.5495(3)	2.6806(3)[b]	2.6802(3)	2.2147(4)	
$Fe_3(CO)_{11}(PPh_3)$[a]	2.558(9)	2.703(9)	2.711(9)	2.25(1)	[52]
	2.568(8)	2.703(9)[b]	2.666(8)	2.24(1)	
$Fe_3(CO)_{12}$	2.558(1)	2.677(2)	2.683(1)	–	[53]

[a] Two independent molecules in the asymmetric unit.
[b] Iron–iron bond *trans* to phosphine.

3. Summary and conclusions

As has been observed for other phosphines containing "pseudo-vinyl" moieties, reaction of PFu_3 or PTh_3 with $[Fe_3(CO)_{12}]$ under mild thermolytic conditions leads to cluster fragmentation and carbon–phosphorus bond cleavage of the ligand to form dinuclear iron carbonyl complexes with $Fe_2(\mu\text{-}\eta^1,\eta^2\text{-}$"pseudo-vinyl")($\mu$-phosphido) cores. In the present case, the clusters $[Fe_2(CO)_6(\mu\text{-}\eta^1,\eta^2\text{-}C_4H_3E)\{\mu\text{-}P(C_4H_3E)_2\}]$ ($E = O$, S) constitute the prototypical products, and mono-phosphine-substituted derivatives of these parent clusters are also observed. At room temperature, the same reaction does not lead to full fragmentation of the trinuclear starting material; thus, small amounts of $[Fe_3(CO)_{11}\{P(C_4H_3E)_3\}]$ ($E = O$, S) are formed. Mild thermolysis of the latter clusters does lead to the formation of $[Fe_2(CO)_6(\mu\text{-}\eta^1,\eta^2\text{-}C_4H_3E)\{\mu\text{-}P(C_4H_3E)_2\}]$ ($E = O$, S) and their phosphine derivatives, as expected, but the rates of these thermolytic reactions are considerably slower than in the direct thermolysis of the parent trinuclear cluster in the presence of the relevant phosphine. This observed difference in reaction rates suggest that a thermolytic pathway proceeding *via* the formation of $[Fe_3(CO)_{11}\{P(C_4H_3E)_3\}]$ ($E = O$, S) as initial products/intermediates, and subsequent decomposition of these neutral intermediates, is not taking place. Rather, it appears that the reaction is free-radical

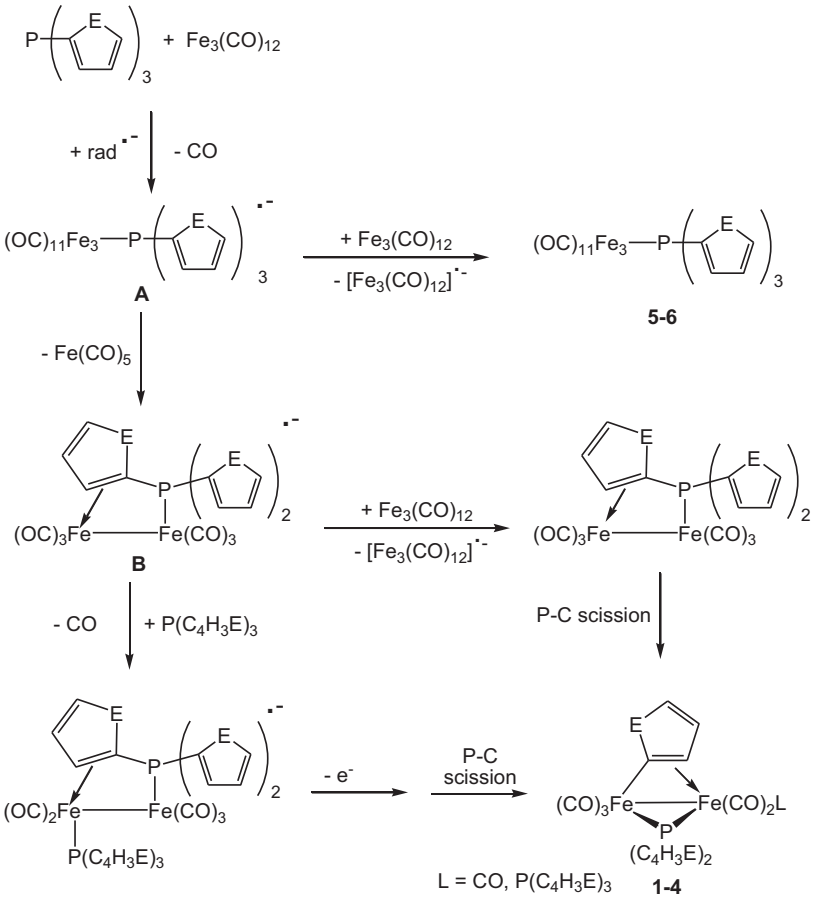

Scheme 4.

initiated; indirect evidence for such a reaction comes from the rapid formation of $[Fe_2(CO)_6(\mu\text{-}\eta^1,\eta^2\text{-Fu})(\mu\text{-}PFu_2)]$ upon addition of a catalytic amount of $Na^+[Ph_2CO]^\bullet$ to $[Fe_3(CO)_{11}(PFu_3)]$. We tentatively propose that the relatively rapid formation of the prototypical dinuclear products in the direct thermolysis of the starting materials may be due to formation of 49-electron radical anions $[Fe_3(CO)_{11}\{P(C_4H_3E)_3\}]^{\bullet-}$, being formed by reduction of $[Fe_3(CO)_{12}]$ or its phosphine-substituted derivatives.

4. Experimental

4.1. General procedures

Unless otherwise stated, purification of solvents, reactions, and manipulation of compounds were carried out under a nitrogen atmosphere with the use of standard Schlenk techniques. All solvents were dried by distillation over appropriate drying agents. The ligands PFu_3 and PTh_3 were purchased from Acros Organics Chemicals Inc. and used without further purification. Methanol-free $[Fe_3(CO)_{12}]$ was prepared by a literature method [65]. All chromatographic separations and ensuing work-up were carried out in open air. Thin layer chromatography was carried out on glass plates pre-coated with Merck 60 0.5 mm silica gel. Infrared spectra were recorded as solutions in 0.5 mm NaCl cells on a Nicolet Avatar 360 FT-IR spectrometer with carbon monoxide as calibrant. Fast atom bombardment (FAB) mass spectra were obtained on a JEOL SX-102 spectrometer using 3-nitrobenzyl alcohol as matrix and CsI as calibrant. Proton and $^{31}P\{^1H\}$NMR spectra were recorded on a Varian Unity 500 MHz NMR spectrometer.

4.1.1. Thermal reaction of $[Fe_3(CO)_{12}]$ with PFu_3

A CH_2Cl_2 solution (30 mL) of $[Fe_3(CO)_{12}]$ (200 mg, 0.40 mmol) and PFu_3 (92 mg, 0.40 mmol) was heated to reflux under a nitrogen atmosphere for 12 h. The solvent was removed under reduced pressure and the residue was chromatographed by TLC on silica gel. Elution with hexane/CH_2Cl_2 (v/v 9:1) developed two bands. The faster moving band afforded light orange $[Fe_2(CO)_6(\mu\text{-}\eta^1,\eta^2\text{-Fu})(\mu\text{-}PFu_2)]$ (**1**) (120 mg, 59%) and the slower moving band gave orange $[Fe_2(CO)_5(\mu\text{-}\eta^1,\eta^2\text{-Fu})(\mu\text{-}PFu_2)(PFu_3)]$ (**2**) (35 mg, 12%).

4.1.1.1. Spectral and analytical data for ***1****.* Anal. Calcd for $C_{18}H_9Fe_2O_9P$: C, 42.23; H, 1.77%. Found: C, 42.26; H, 1.80%. IR (ν(CO), CH_2Cl_2): 2069 s, 2033 vs. 1999 s, 1988 s cm^{-1}. ^1H NMR ($CDCl_3$): δ 7.83 (m, 1H), 7.68 (m, 2H), 6.72 (m, 1H), 6.54 (m, 1H), 6.42 (m, 2H), 6.09 (m, 1H), 4.18 (dd, $J = 7.2$ Hz, 1H). $^{31}P\{^1H\}$ NMR ($CDCl_3$): 91.7 (s). ESI-MS: m/z 512 $[M^+]$.

4.1.1.2. Spectral and analytical data for ***2****.* Anal. Calcd for $C_{29}H_{18}Fe_2O_{11}P_2$: C, 48.64; H, 2.53%. Found: C, 48.66; H, 2.57%. IR ν(CO), CH_2Cl_2): 2046 vs, 1997 s, 1981 m, 1965 w cm^{-1}. ^1H NMR ($CDCl_3$): δ 7.71 (m, 1H), 7.65 (m, 1H), 7.54 (m, 3H), 7.42 (m, 1H), 6.55 (m, 3H), 6.52 (m, 1H), 6.39 (m, 4H), 6.19 (m, 1H), 6.14 (m, 1H), 5.75 (m, 1H), 4.22 (m, 1H). $^{31}P\{^1H\}$ NMR ($CDCl_3$): 80.9 (d), 21.3 (d, $J = 29.1$ Hz). ESI-MS: m/z 716 $[M^+]$.

4.1.2. Reaction of $[Fe_3(CO)_{12}]$ with PFu_3 at room temperature

A CH_2Cl_2 solution (3 mL) of $[Fe_3(CO)_{12}]$ (200 mg, 0.40 mmol) and PFu_3 (92 mg, 0.40 mmol) was stirred at room temperature under a nitrogen atmosphere for 18 h. The solvent was removed under

reduced pressure and the residue was purified by TLC on silica gel. Elution with hexane/CH_2Cl_2 (v/v 9:1) developed five bands. The first band was green unreacted [$Fe_3(CO)_{12}$] (trace). The second to fourth band afforded the following compounds in order of elution: **1** (115 mg, 57%), **2** (30 mg, 11%) and $Fe_3(CO)_{11}(PFu_3)$ (**5**) (15 mg, 6%) as green crystals after recrystallization from hexane/CH_2Cl_2 at −20 °C.

*4.1.2.1. Spectral and analytical data for **5**.* Anal. Calcd for $C_{23}H_9Fe_3O_{14}P$: C, 39.02; H, 1.28%. Found: C, 39.08; H, 1.31%. IR (ν(CO), CH_2Cl_2): 2085 s, 2033 s, 2010 s, 1847 w, 1807 w cm^{-1}. ^1H NMR ($CDCl_3$): δ 7.75 (m, 3H), 6.67 (m, 3H), 6.50 (m, 3H). $^{31}P\{^1H\}$ NMR ($CDCl_3$): 20.0 (s). ESI-MS: m/z 708.80 $[M + Na]^+$ (calc. 731.10).

4.1.3. Reaction of 1 with PFu_3

A CH_2Cl_2 solution (15 mL) of **1** (30 mg, 0.059 mmol) and PFu_3 (14 mg, 0.059 mmol) was heated to reflux under a nitrogen atmosphere for 6 h. The solvent was removed under reduced pressure and the residue was chromatographed by TLC on silica gel. Elution with hexane/CH_2Cl_2 (v/v 9:1) developed two orange bands giving unreacted **1** (20 mg, 67%) and **2** (4 mg, 10%).

4.1.4. Thermolysis of 5

A CH_2Cl_2 solution (15 mL) of **5** (20 mg, 0.028 mmol) was heated to reflux under a nitrogen atmosphere for 5 h. The solvent was removed under reduced pressure and the residue was chromatographed by TLC on silica gel. Elution with hexane/CH_2Cl_2 (v/v 9:1) developed two bands which gave **1** (5 mg, 35%) and **2** (3 mg, 15%).

4.1.5. Reaction of 5 with sodium benzophenone-ketyl

To a thf solution (15 mL) of **5** (20 mg, 0.028 mmol) was added 1–2 drops of a thf solution of sodium benzophenone-ketyl (BPK) and the mixture was stirred at room temperature for 1 h. The solvent was removed under reduced pressure and the residue chromatographed by TLC on silica gel. Elution with hexane/CH_2Cl_2 (v/v 9:1) developed two bands. The faster moving band afforded **1** (10 mg, 62%) and the slower moving band was green unreacted starting material (trace). A similar treatment of **5** in thf for 2 h but without the addition of BPK followed by chromatographic separation as above afforded only unreacted **1** almost quantitatively.

4.1.6. Thermal reaction of [$Fe_3(CO)_{12}$] with PTh_3

A CH_2Cl_2 solution (30 mL) of [$Fe_3(CO)_{12}$] (200 mg, 0.40 mmol) and PTh_3 (111 mg, 0.40 mmol) was heated to reflux for 12 h. The solvent was removed under reduced pressure and the residue chromatographed by TLC on silica gel. Elution with hexane/CH_2Cl_2 (v/v 9:1) developed two bands [$Fe_2(CO)_6(\mu\text{-}\eta^1,\eta^2\text{-Th})(\mu\text{-}PTh_2)$] (**3**) (160 mg, 72%) as light orange crystals and [$Fe_2(CO)_5(\mu\text{-}\eta^1,\eta^2\text{-Th})(\mu\text{-}PTh_2)(PTh_3)$] (**4**) (6 mg, 2%) as deep orange crystals.

*4.1.6.1. Spectral and analytical data for **3**.* Anal. Calcd for $C_{18}H_9Fe_2O_6PS_3$: C, 38.59; H, 1.62. Found: C, 38.65; H, 1.64%. IR (ν(CO), CH_2Cl_2): 2063 s, 2030 vs., 1988 s cm^{-1}. ^1H NMR ($CDCl_3$): δ 7.72 (m, 1H), 7.61 (m, 2H), 7.49 (m, 1H), 7.15 (m, 1H), 7.10 (m, 1H), 6.99 (m, 1H), 6.80 (m, 1H), 4.65 (m, 1H). $^{31}P\{^1H\}$ NMR ($CDCl_3$): 113.0 (s). ESI-MS: m/z 560 [M^+].

*4.1.6.2. Spectral and analytical data for **4**.* Anal. Calcd for $C_{29}H_{18}Fe_2O_5P_2S_6$: C, 42.87; H, 2.23. Found: C, 42.91; H, 2.25%. IR (ν(CO), CH_2Cl_2): 2038 vs, 1985 s, 1952 w, and 1945 w cm^{-1}. ^1H NMR ($CDCl_3$): δ 7.78–7.35 (m, 6H), 6.55–5.96 (m, 10H), 5.56 (m, 1H), 4.24 (m, 1H). $^{31}P\{^1H\}$ NMR ($CDCl_3$): 75.9 (d), 23.2 (d, $J = 26.2$ Hz).

Table 3
Crystal data and experimental details for [$Fe_2(CO)_6(\mu\text{-}\eta^1,\eta^2\text{-Fu})(\mu\text{-}PFu_2)$] (**1**), [$Fe_2(CO)_5(\mu\text{-}\eta^1,\eta^2\text{-Fu})(\mu\text{-}PFu_2)(PFu_3)$] (**2**), [$Fe_2(CO)_6(\mu\text{-}\eta^1,\eta^2\text{-Th})(\mu\text{-}PTh_2)$] (**3**) and [$Fe_3(CO)_9(\mu\text{-}CO)_2(PFu_3)$] (**5**).

Compound	**1**	**2**	**3**	**5**
Empirical formula	$C_{18}H_9O_9Fe_2P_1$	$C_{29}H_{18}O_{11}Fe_2P_2$	$C_{18}H_9O_6Fe_2S_3P_1$	$C_{23}H_9O_{14}Fe_3P_1$
Formula weight	511.92	1432.15	560.10	707.82
Temp (K)	150(2)	150(2)	150(2)	100(2)
Wavelength (Å)	0.71073	0.71073	0.71073	0.71073
Crystal system	Orthorhombic	Monoclinic	Monoclinic	Monoclinic
Space group	P $2_12_12_1$	$P2_1/c$	$P2_1/n$	$P2_1/c$
a (Å)	8.247(2)	20.746(2)	9.563(1)	8.4956(2)
b (Å)	15.385(3)	16.282(15)	12.430(2)	16.442(4)
c (Å)	15.444(3)	18.335(17)	17.645(2)	37.182(8)
α (°)	90	90	90	90
β (°)	90	109.51(2)	95.745(2)	94.291(1)
γ (°)	90	90	90	90
Volume (Å^3)	1959.6(7)	5837.9(9)	2086.9(4)	5179.2(2)
Z	4	4	4	8
D_{calc} (Mg m^{-3})	1.735	1.629	1.783	1.816
μ (Mo Kα) (mm^{-1})	1.612	1.165	1.800	1.793
F(000)	1024	2896	1120	2816
Crystal colour	Orange	Orange	Orange	Green
Crystal size (mm)	0.28 × 0.14 × 0.12	0.26 × 0.26 × 0.12	0.16 × 0.08 × 0.03	0.36 × 0.26 × 0.09
θ range (°)	2.65–28.26	1.72–28.29	2.01–28.33	2.22–28.31
Limiting indices	$-10 \le h \ge 10$	$-26 \le h \ge 26$	$-12 \le h \ge 12$	$-32 \le h \ge 33$
	$-20 \le k \ge 20$	$-21 \le k \ge 21$	$-16 \le k \ge 16$	$-17 \le k \ge 17$
	$-20 \le l \ge 20$	$-23 \le l \ge 23$	$-22 \le l \ge 23$	$-39 \le l \ge 39$
Structure solution	Direct methods	Direct methods	Direct methods	Direct methods
Reflections collected	16,746	13,940	17,653	74,733
Independent reflections (R_{int})	4704 (0.0487)	8750 (0.0677)	4960 (0.0542)	19832 (0.0313)
Max. and min. transmission	0.8301 and 0.6611	0.8728 and 0.7515	0.9480 and 0.7616	0.8496 and 0.5670
Data/restraints/parameters	4704/0/307	13940/0/793	4960/0/274	19832/0/739
Goodness of fit on F^2	0.989	0.957	1.015	1.026
Final R indices [$I > 2\sigma(I)$]	$R_1 = 0.0328$	$R_1 = 0.0508$	$R_1 = 0.0480$	$R_1 = 0.0318$
	$wR_2 = 0.0622$	$wR_2 = 0.1056$	$wR_2 = 0.1022$	$wR_2 = 0.0610$
R indices (all data)	$R_1 = 0.0385$	$R_1 = 0.0915$	$R_1 = 0.0749$	$R_1 = 0.0480$
	$wR_2 = 0.0644$	$wR_2 = 0.1202$	$wR_2 = 0.1106$	$wR_2 = 0.0652$
Largest peak and hole (e Å^{-3})	0.447 and −0.348	0.837 and −0.526	0.965 and −0.955	0.558 and −0.402

4.1.7. Reaction of $[Fe_3(CO)_{12}]$ with PTh_3

A CH_2Cl_2 solution (30 mL) of $[Fe_3(CO)_{12}]$ (200 mg, 0.40 mmol) and PTh_3 (111 mg, 0.40 mmol) was at room temperature under a nitrogen atmosphere for 24 h. The solvent was removed under reduced pressure and the residue chromatographed by TLC on silica gel. Elution with hexane/CH_2Cl_2 (v/v 9:1) developed five bands. The first band was green unreacted starting material (trace). The second to fourth band afforded the following compounds in order of elution: **3** (130 mg, 58%) and **4** (5 mg, 2%) and $[Fe_3(CO)_{11}(PTh_3)]$ (**6**) (20 mg, 7%) as green crystals after recrystallization from hexane/CH_2Cl_2 at −20 °C. The fourth band gave too little product for complete characterization.

*4.1.7.1. Spectral and analytical data for **6**.* Anal. Calcd for $C_{23}H_9Fe_3O_{11}PS_3$: C, 36.53; H, 1.20%. Found: C, 36.60; H, 1.25%. IR (ν(CO), CH_2Cl_2): 2085 s, 2034 s, 2010 vs, 1840w. 1800w cm^{-1}. ^1H NMR ($CDCl_3$): δ 7.65 (m, 5H), 7.46 (m, 4H), $^{31}P\{^1H\}$ NMR ($CDCl_3$): 33.0 (s), ESI-MS: *m/z* 756.89 $[M + Na]^+$ (calc. 778.69).

4.1.8. Thermolysis of 6

A CH_2Cl_2 solution (15 mL) of **6** (20 mg, 0.026 mmol) was heated to reflux under a nitrogen atmosphere for 6 h. The solvent was removed under reduced pressure and the residue was chromatographed by TLC on silica gel. Elution with hexane/CH_2Cl_2 (v/v 9:1) developed two bands. The faster moving band afforded light orange **3** (6 mg, 40%) while the slower moving band gave too little product for complete characterization.

4.1.9. X-ray crystallography

Single crystals of **1**–**3** were mounted on fibres and diffraction data collected at 150 K on a Bruker SMART APEX diffractometer using Mo-Kα radiation ($\lambda = 0.71073$ Å). Data collection, indexing and initial cell refinements were all done using SMART software. Data reduction was accomplished with SAINT software and SADABS programs were used to apply empirical absorption corrections. The structures were solved by direct methods or Patterson methods and refined by full matrix least-squares. All non-hydrogen atoms were refined anisotropically and hydrogen atoms were included using a riding model. In **3** one of the thienyl rings is disordered over two sites (70:30) S2/S2A and C12/C12A. Due to this disorder these atoms were refined only isotropically and the proton was not added to C12/C12A. Scattering factors were taken from International Tables for X-ray Crystallography. The diffraction data for **5** were collected at 100 K using a Bruker AXS, 2010 Kappa ApexII Duo diffractometer with Mo-Kα radiation ($\lambda = 0.71073$ Å). The SAINT (Bruker AXS, 2009) program packages were used for cell refinements and data reduction. The structure solutions were carried out using the SHELXS97 program with the CrystaMaker (CrystaMaker software Ltd., 2011) graphical user interface. Hydrogen atoms were positioned geometrically and were also constrained to ride on their parent atoms. Details of data collection and structure refinement are given in Table 3.

Acknowledgements

This research has been part sponsored by the European Union (an Erasmus Mundus Scholarship to AR) and Ministry of Science and Information & Communication Technology, Government of the People's Republic of Bangladesh. We thank the Commonwealth Scholarship Commission for the award of a Commonwealth Scholarship to SG. We are grateful to the helpful comments of one referee for suggesting the Na[Ph_2CO] initiated reaction.

Appendix A. Supplementary material

CCDC Nos. 904053–90456 contain the supplementary crystallographic data for this paper. These data can be obtained free of charge from The Cambridge Crystallographic Data Centre *via* www.ccdc.cam.ac.uk/data_request/cif.

References

[1] W.-Y. Wong, F.-L. Ting, W.-L. Lam, Eur. J. Inorg. Chem. (2002) 2103–2111.
[2] W.-Y. Wong, F.-L. Ting, Z. Lin, Organometallics 22 (2003) 5100–5108.
[3] N.G. Anderson, B.A. Keay, Chem. Rev. 101 (2001) 997–1030.
[4] M. Sakai, H. Hayashi, N. Miyaura, Organometallics 16 (1997) 4229–4231.
[5] E. Shirakawa, K. Yamasaki, T. Hiyama, Synthesis (1998) 1544–1549.
[6] B.M. Trost, Y.H. Rhee, J. Am. Chem. Soc. 121 (1999) 11680–11683.
[7] J.C. Anderson, H. Namli, C.A. Roberts, Tetrahedron 53 (1997) 15123–15134.
[8] W.A. Herrmann, S. Brossmer, K. Öfele, M. Beller, H. Fischer, J. Mol. Catal. A: Chem. 103 (1995) 133–146.
[9] V. Farina, S.R. Baker, D.A. Benigni, C. Sapino, Tetrahedron Lett. 29 (1988) 5739–5742.
[10] I. Klement, M. Rottländer, C.E. Tucker, T.N. Majid, P. Knochel, P. Venegas, G. Cahiez, Tetrahedron 52 (1996) 7201–7220.
[11] S. Ghosh, M. Khatun, D.T. Haworth, S.V. Lindeman, T.A. Siddiquee, D.W. Bennett, G. Hogarth, E. Nordlander, S.E. Kabir, J. Organomet. Chem. 694 (2009) 2941–2948.
[12] S. Karmaker, S. Ghosh, S.E. Kabir, D.T. Haworth, S.V. Lindeman, Inorg. Chim. Acta 382 (2012) 199–202.
[13] Md.A. Rahman, N. Begum, S. Ghosh, Md. K. Hossain, G. Hogarth, D.A. Tocher, E. Nordlander, S.E. Kabir, J. Organomet. Chem. 696 (2011) 607–612.
[14] C. Santelli-Rouvier, C. Coin, L. Toupet, M. Santelli, J. Organomet. Chem. 495 (1995) 91–96.
[15] W.-Y. Wong, F.-L. Ting, W.-L. Lam, J. Chem. Soc. Dalton Trans. (2001) 2981–2988.
[16] N. Begum, M.A. Rahman, M.R. Hassan, S.E. Kabir, E. Nordlander, G. Hogarth, D.A. Tocher, J. Organomet. Chem. 693 (2008) 1645–1655.
[17] S. Ghosh, G. Hogarth, S.E. Kabir, E. Nordlander, L. Salassa, D.A. Tocher, J. Organomet. Chem. 696 (2011) 1982–1989.
[18] Md.I. Hossain, Md.D.H. Sikder, S. Ghosh, S.E. Kabir, G. Hogarth, L. Salassa, Organometallics 31 (2012) 2546–2558.
[19] S. Ghosh, S. Rana, D.A. Tocher, G. Hogarth, E. Nordlander, S.E. Kabir, J. Organomet. Chem. 694 (2009) 3312–3319.
[20] Md.N. Uddin, N. Begum, Md.R. Hassan, G. Hogarth, S.E. Kabir, Md.A. Miah, E. Nordlander, D.A. Tocher, J. Chem. Soc. Dalton Trans. (2008) 6219–6230.
[21] U. Bodensieck, H. Vahrenkamp, G. Rheinwald, H. Stoeckli-Evans, J. Organomet. Chem. 488 (1995) 85–90.
[22] N.K. Kiriakidou Kazemifar, M.J. Stchedroff, M.A. Mottalib, S. Selva, M. Monari, E. Nordlander, Eur. J. Inorg. Chem. (2006) 2058–2068.
[23] A.J. Deeming, M.K. Shinmar, A.J. Arce, Y. De. Sanctis, J. Chem. Soc. Dalton Trans. (1999) 1153–1160.
[24] A.J. Deeming, S.N. Jayasuriya, A.J. Arce, Y. De. Sanctis, Organometallics 15 (1996) 786–793.
[25] M.A. Mottalib, S.E. Kabir, D.A. Tocher, A.J. Deeming, E. Nordlander, J. Organomet. Chem. 692 (2007) 5007–5016.
[26] J.D. King, M. Monari, E. Nordlander, J. Organomet. Chem. 573 (1999) 272–278.
[27] Md.N. Uddin, M.A. Mottalib, N. Begum, S. Ghosh, A.K. Raha, D.T. Haworth, S.V. Lindeman, T.A. Siddiquee, D.W. Bennett, G. Hogarth, E. Nordlander, S.E. Kabir, Organometallics 28 (2009) 1514–1523.
[28] S. Ghosh, G. Hogarth, D.A. Tocher, E. Nordlander, S.E. Kabir, Inorg. Chim. Acta 363 (2010) 1611–1614.
[29] S. Ghosh, A.K. Das, N. Begum, D.T. Haworth, S.V. Lindeman, J.F. Gardinier, T.A. Siddiquee, D.W. Bennett, E. Nordlander, G. Hogarth, S.E. Kabir, Inorg. Chim. Acta 362 (2009) 5175–5182.
[30] M. Ackermann, A. Pascariu, T. Höcher, H.-U. Siehl, S. Berger, J. Am. Chem. Soc. 128 (2006) 8434–8440.
[31] M.K. Anwar, G. Hogarth, O.S. Senturk, W. Clegg, S. Doherty, M.R.J. Elsegood, J. Chem. Soc. Dalton Trans. (2001) 341–352.
[32] R. Yáñez, J. Ros, R. Mathieu, X. Solans, M. Font-Bardia, J. Organomet. Chem. 389 (1990) 219–226.
[33] S.A. MacLaughlin, S. Doherty, N.J. Taylor, A.J. Carty, Organometallics 11 (1992) 4315–4325.
[34] G. Hogarth, M.H. Lavender, J. Chem. Soc. Dalton Trans. (1992) 2759–2764.
[35] G. Hogarth, M.H. Lavender, K. Shukri, J. Organomet. Chem. 527 (1997) 247–258.
[36] G. Hogarth, K. Shukri, S. Doherty, A.J. Carty, G.D. Enright, Inorg. Chim. Acta 291 (1999) 178–189.
[37] G. Hogarth, M.H. Lavender, K. Shukri, Organometallics 14 (1995) 2325–2341.
[38] T. Fässler, G. Huttner, J. Organomet. Chem. 376 (1989) 367–384.
[39] R. Yañez, J. Ros, X. Solans, M. Font-Bardia, J. Organomet. Chem. 395 (1990) 305–314.
[40] R. Reina, O. Rossell, M. Seco, J. Ros, R. Yáñez, A. Perales, Inorg. Chem. 30 (1991) 3973–3976.
[41] J. Ros, J.M. Viñas, R. Mathieu, X. Solans, M. Font-Bardia, J. Chem. Soc. Dalton Trans. (1988) 281–284.
[42] X.-K. Yao, R.-J. Wang, H.-G. Wang, L.-S. Song, Q.-M. Hu, J.-T. Wang, Acta Crystallogr. Sect. C 45 (1989) 575–579.
[43] J. Ros, J.M. Viñas, R. Mathieu, X. Solans, M. Font-Bardia, J. Organomet. Chem. 307 (1986) C7–C9.

[44] D. Seyferth, L.L. Anderson, F. Villafane, M. Cowie, R.W. Hilts, Organometallics 11 (1992) 3262–3271.
[45] N.M. Doherty, G. Hogarth, S.A.R. Knox, K.A. Macpherson, F. Melchior, A.G. Orpen, J. Chem. Soc. Chem. Commun. (1986) 540–542.
[46] N.J. Grist, G. Hogarth, S.A.R. Knox, B.R. Lloyd, D.A.V. Morton, A.G. Orpen, J. Chem. Soc. Chem. Commun. (1988) 673–675.
[47] G. Hogarth, S.A.R. Knox, M.L. Turner, J.Chem. Soc. Chem. Commun. (1990) 145–146.
[48] N.M. Doherty, G. Hogarth, S.A.R. Knox, K.A. Macpherson, F. Melchior, D.A.V. Morton, A.G. Orpen, Inorg. Chim. Acta 198-200 (1992) 257–270.
[49] G. Hogarth, S.P. Redmond, J. Organomet. Chem. 534 (1997) 221–227.
[50] P. Das, M. Borah, F. Michaud, F.Y. Pétillon, P. Schollhammer, Inorg. Chim. Acta 376 (2011) 641–644.
[51] G. Hogarth, J. Organomet. Chem. 407 (1991) 91–95.
[52] D.J. Dahm, R.A. Jacobson, J. Am. Chem. Soc. 90 (1968) 5106–5112.
[53] F.A. Cotton, J.M. Troup, J. Am. Chem. Soc. 96 (1974) 4155–4159.
[54] D. Braga, F. Grepioni, L.J. Farrugia, B.F.G. Johnson, J. Chem. Soc. Dalton Trans. (1994) 2911–2918.
[55] A. Shojale, J.D. Atwood, Organometallics 4 (1985) 187–190.
[56] R. Kumar, J. Organomet. Chem. 136 (1977) 235–239.
[57] F.-H. Luo, S.-R. Yang, C.-S. Li, J.-P. Duan, C.-H. Cheng, J. Chem. Soc. Dalton Trans. (1991) 2435–2439.
[58] M.I. Bruce, D.C. Kehoe, J.G. Matisons, B.K. Nicholson, P.H. Rieger, M.L. Williams, J. Chem. Soc. Chem. Commun. (1982) 442–444.
[59] Y.A. Belousov, T.A. Belousova, Polyhedron 18 (1999) 2605–2608.
[60] P.A. Dawson, B.M. Peake, B.H. Robinson, J. Simpson, Inorg. Chem. 19 (1980) 465–472.
[61] A.J. Downard, B.H. Robinson, J. Simpson, A.M. Bond, J. Organomet. Chem. 320 (1983) 363–384.
[62] F. Ragaini, D.L. Ramage, J.-S. Song, G.L. Geoffroy, J. Am. Chem. Soc. 115 (1993) 12183–12184.
[63] S.M. Grant, A.R. Manning, Inorg. Chim. Acta 31 (1978) 41–48.
[64] http://www.sigmaaldrich.com/chemistry/solvents/learning-center/stabilizer-systems.html.
[65] W. McFarlane, G. Wilkinson, Inorg. Synth. 8 (1965) 181–183.